Design and Implementation of Zeabus AUV for Robosub 2017

Vasutorn Siriyakorn, Supakit Kriangkajorn, Natchanan Thongtem, Thanathat Patthapong, and Monpriya Tammavong

***Abstract*—Kasetsart University has participated in Robosub since 2014. In 2017, our AUV called Zeabus has been redesigned in a single hull with a truss structure and acrylic covers to reduce weight. More advanced equipment such as imaging sonar and new cameras are added. More features of software parts are also improved such as auto exposure and new object detection algorithms in order to perform tasks more efficiently. Devices, computers, and main circuits have been installed in a single hull. Circuit boards are redesigned to reduce the size and weight. Thrusters have been replaced by Seabotix BTD 150, and driver circuits have been redesigned to support our new thrusters. Zeabus AUV is still operated on *ROS (Robot Operating System)* like in the previous version.**

I. Introduction

Robosub is an international AUV competition organized by AUVSI (Association for Unmanned Vehicle System International) foundation and is co-sponsored by ONR (Office of Naval Research). The competition is annually held at TRANSDEC facility, part of SPAWAR Systems Center Pacific in San Diego, California. The competition is designed to challenge student-built AUVs with tasks that simulate real-world missions.

The Faculty of Engineering, Kasetsart University, has participated in Robosub since 2014. Our team continue to improve the team AUV every year. As a result, the ranking of our team named as Zeabus has kept improving from 18th in 2014, 10th in 2015, and 5th in the final round of 2016. The name of our AUV is Zeabus, which is the same as our team's name. In 2017, our team has significantly redesigned Zeabus to improve the overall performance and aimed for a better result in the competition. The overall design strategy is explained in Section II. Section III describes mechanical design of AUV. Section IV explains electrical design including electrical structures and sensors used. Section V provides information of software implemented for AUV control and navigation. Section VI shows some experimental results. Finally, section VII ends the paper with the conclusion.

II. Design Strategy

Based on our experience in 2016, we have found many problems in our design as follows.

1) Overweight

In 2016, although a single hull concept is proven to be successful based on our competition result, our previous design is slightly overweight and our score was reduced due to the weight. Thus, our main object of AUV body design is to reduce the weight as much as possible. Our strategy in this case is to reduce the size of the AUV, use lighter materials, and implement a better mechanical structure design based on aluminum and acrylic materials. We expected that our vehicle can contains all equipment, of which the number is more than the previous year, but with the less total weight.

2) Sizes of electronics

Sizes of electronics were also matters. In 2016, several electronic circuit boards and equipment are off-the-shelf products, whose sizes cannot be modified and typically unnecessarily large. Because of their sizes, the AUV in the previous has to be large enough to contain these equipment, which implies more weight. Thus, in this year, our strategy for electronic design is to build custom PCBs, which can reduce sizes to be contained in the main hull.

3) Vision system

In the previous year, our vision system did not perform well under the bright sunlight. We have planned to improve the performance of our vision system by using more advance image processing algorithms.

In addition, we added an image sonar to collaborate with the vision system for AUV navigation. This is a new equipment for our team.

Other than these technical problems, we also have management problems such as limited team members, testing time, and sponsorship. Many technical members have already graduated. To solve team member problems, we recruited and trained several new members as many as possible. In order to handle our limited sponsorship problem, we have reduced some designs and equipment so we can build the new AUV with a limited budget. However, our limited testing time due to student studying schedules is unavoidable so we have to test our AUV as much as we can do.

III. Mechanical Design

A. Overall

In this year, our mechanical team focuses on establishing systematic mechanical design procedures. From the last year, we have done additional research on correlations between mechanical components and the robustness of the system. We laid out all components to achieve roll stability and position horizontal thrusters in alignment with the center of gravity's plane. Buoyancy of the vehicle is slightly positive. We set main goals for the design as follows; weight reduction, sealing, flexibility and service. Eventually, we are

able to reduce the overall weight up to 40%, determine the center of gravity and inertia parameters, and improve the vehicle stability over the last year. The new Zeabus platform is shown in Fig. 1.

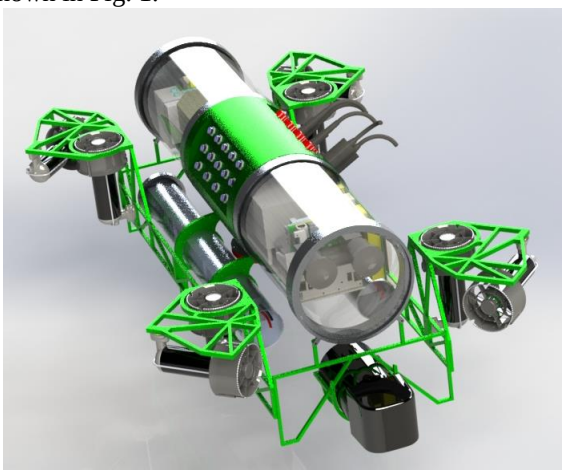

Fig.1. Zeabus generation III platform.

Materials used to build the Zeabus platform are aluminum, acrylic and ABS plastic.

B. Main hull

In this year, we use a single hull design. The main hull contains all main electrical components. We emphasize on weight reduction and manufacturability. It is designed to have 3 planar surfaces on the cylinder-shaped hull for all pneumatic, electrical and communication connecters, a DVL plug, and a hydrophone plug. A primary design of the main hull was reconsidered to be implementable on a 4-axis CNC turning machine and a 3-axis milling machine. Welding is selected as a method to connect DVL and hydrophone plugs with the main hull. The main hull is sealed with 2 cylindrical acrylic plugs by means of bore sealing for ease of assembling. Acrylic plastic is used to build clear front and back of the main hull, which allows us to integrate the whole camera system within the single hull by using its transparent property.

C. Frame

The frame shown as the green frame in Figure. 1 holds all components of the vehicle together and gives robustness and rigidity to the vehicle. We apply a concept of space frame to the design. Aluminum is chosen as a material for the frame due to its strength, light weight and corrosion resistance. The frame is designed to be 2-D profiles for water jet machining. All sub-parts of the frame are connected by bolts and welding. The design can achieve 50-percent weight reduction from the last year.

D. Battery pods

Battery pods are designed to have less cross section area and volume in order to reduce drag and buoyancy as shown in Figure 2. This is the same design used in Robosub 2016.

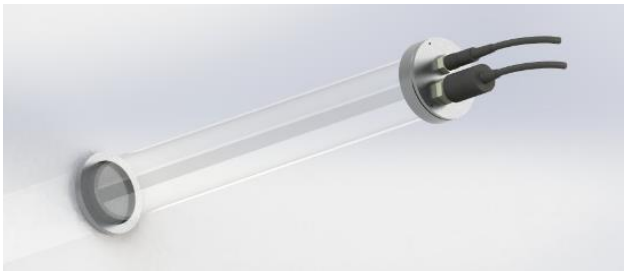

Fig. 2. New battery pod.

E. Gripper

A pneumatic gripper is made of aluminum and 3D printed plastic to reduce the weight. This gripper shown in Fig. 3 is installed at the back of the AUV.

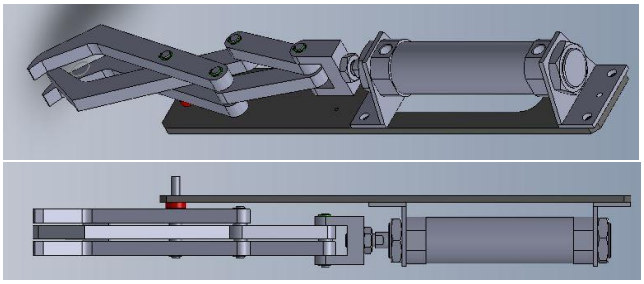

Fig. 3. Gripper

F. Torpedo launcher

A Zeabus torpedo launcher shown in Fig. 4 was made of a PVC pipe. A torpedo can be launched with a power of a spring inside a launcher. A pneumatic lock is used to block a torpedo. In order to fire a torpedo, this lock is released and the torpedo will be launched with a potential energy from a spring. Another torpedo launcher is used as a marker dropper. When Zeabus wants to drop a marker, the AUV just fires a torpedo downward to the target. Torpedoes were made of ABS. Since the density of ABS is close to water, a fired torpedo will not be significantly affected by buoyancy and can hit a target with more accuracy.

Fig. 4. Torpedo launcher.

G. Pneumatic system

A pneumatic system is used to drive a gripper, fire a torpedo, and drop a marker. It is built by using SMC SY3100 U1 solenoid valves shown in Fig. 5, which are connected with a disposable CO_2 cartridge.

Fig. 5. SMC SY3100 U1 solenoid valves

H. Thrusters

Eight Blue Robotics T200-R1 are used as a vehicle's thruster on the 2016 platform because of their high thrust and light weight. Four of eight thrusters are mounted along the vertical axis to provide a high downward thrust, and the remaining thrusters are mounted by 45 degree along the vehicle to provide a thrust on the xy coordinate.

IV. Electrical Design

A. Electrical Architecture

Electrical parts of Zeabus AUV are divided into several modules so that they can be manufactured, tested, maintained, or upgraded separately without affecting other subsystems. With this design concept, the system up-time can be maximized. Main design concerns of these modules are safety, ease of uses, low energy consumption, low weight, and high reliability. Also, the sizes of these modules must be fitted in limited installation areas. Electrical modules implemented on Zeabus are shown in Fig. 6 and listed as follows.

1) Power distribution modules

This module mainly transfers the power from batteries to all other modules. The module is able to protect the overall system when an overcurrent is drawn. The module will shut down the whole system if the emergency switch is activated. The power distribution module also includes many isolated voltage regulators to supply power to sensors, computers, and other modules that require a stable power source.

2) Thruster controller module

This module controls all 8 thrusters by receiving commands from an on-board computer and generates control signals to Electronics Speed Controllers (ESC).

3) Communication bridge module

This module converts signals from serial ports to USB in order to connect serial communication to an on-board computer. This module also provides signal isolation on transmitted and received signals to reduce communication noises.

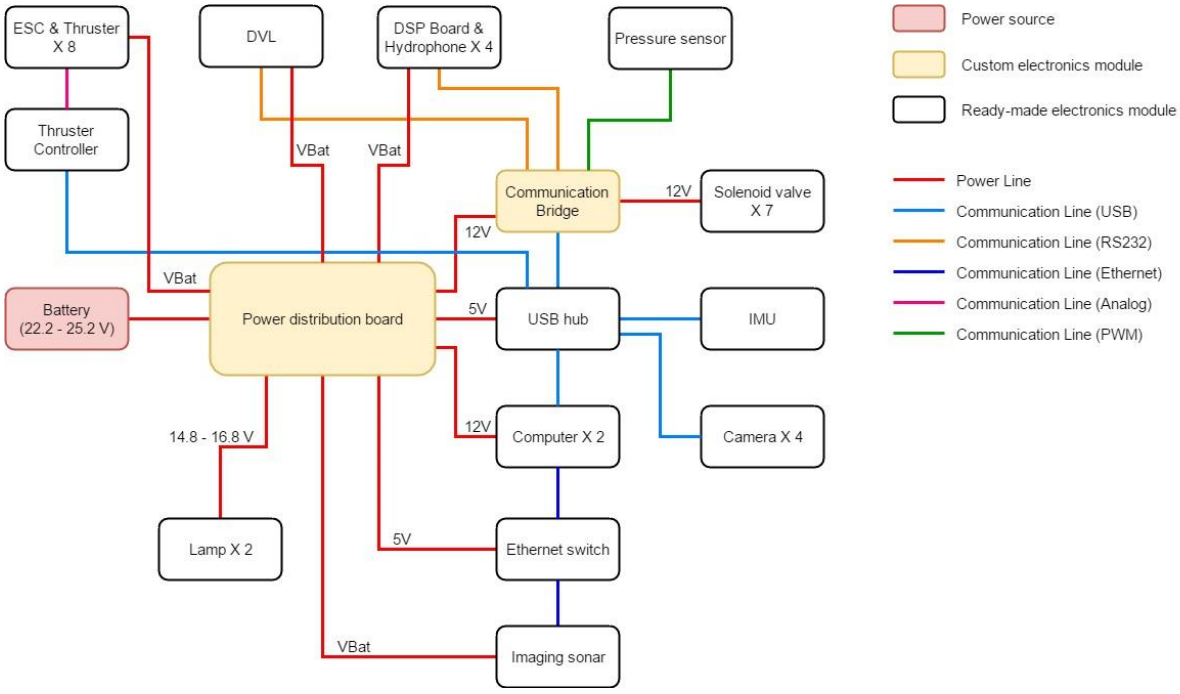

Fig. 6. Electrical modules and connections

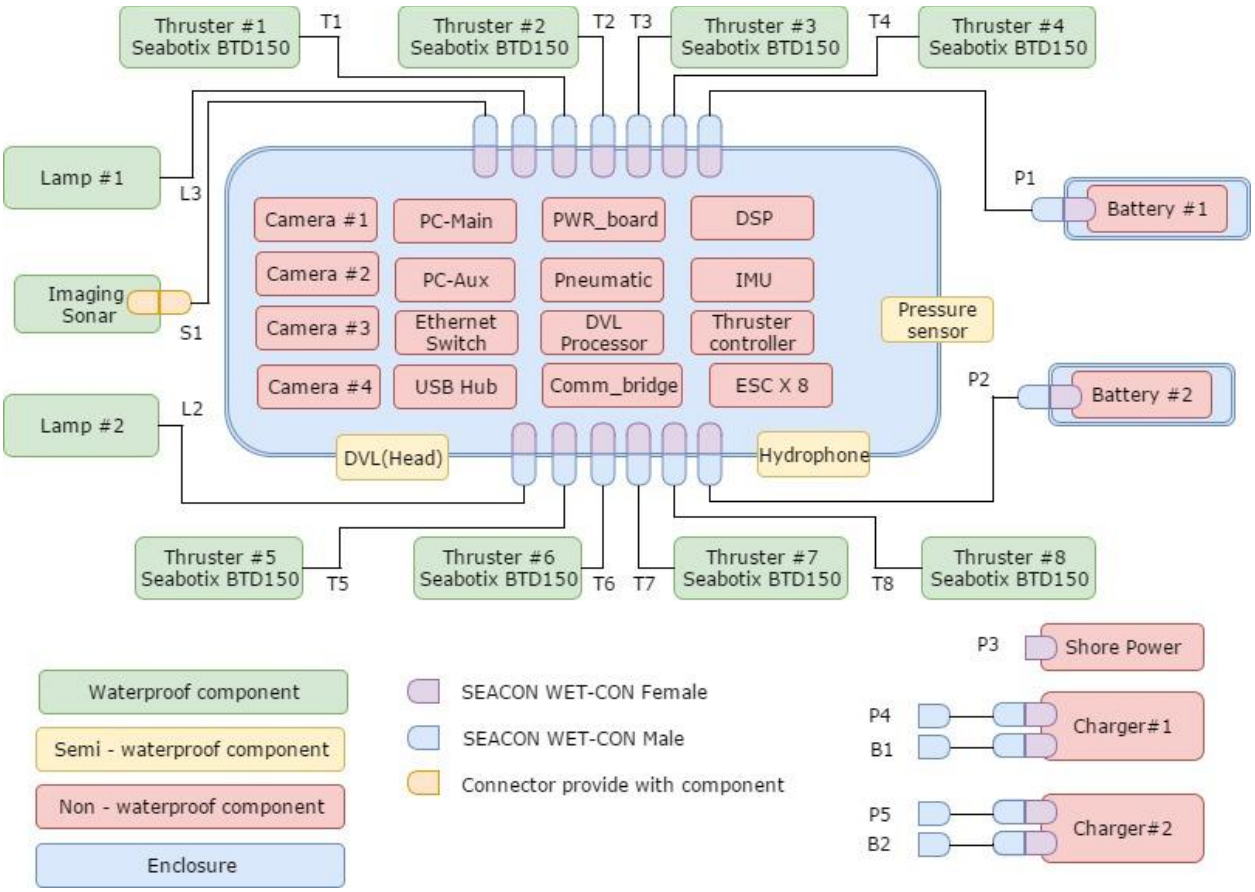

Fig. 7. External connections and diagram.

B. Connectors

Zeabus AUV connections use SEACON WET-CON IL, MCIL-series connectors to connect thrusters, external batteries, Ethernet network, and lamps. SEACON connectors are specially designed for underwater environment and can be mated in wet condition. These connections are shown in Fig. 7.

C. Computers and peripherals

There are several computers and peripherals used in the Zeabus AUV as follows:

1) Main PC

The main computer used to control Zeabus AUV is Intel NUC6I5SYK as shown in Fig. 8.

Fig. 8 Main computer Intel NUC6I5SYK.

2) Auxiliary PC

This PC is used to process computer vision tasks and also serves as a backup computer. If there is any wrong, we can replace the main PC with the auxiliary PC with slightly degraded performance. However, the overall system still be able to work.

3) Ethernet switch

An Ethernet switch used for communication in Zeabus AUV is D-Link DGS-105 shown in Fig. 9. This switch is used because of its speed, small size, and metal housing to reduce noises and enable heat dissipation.

Fig. 9. D-Link DGS-105

4) Shorepower

This is a power supply used when the AUV is not in water. When the AUV is put on the water, the power cables supplied by Shorepower can be taken out without any interruption on the AUV operation. The power supply used as Shorepower is MEANWELL SE-600-24.

5) USB hub

A USB hub used for data transfer in AUV is Orico H4818-U3.

Fig. 10. Orico H4818-U3

D. Sensors

There are several sensors used on Zeabus AUV as follows:

1) Cameras

The camera model used in the AUV is IDS UI-3260CP-C-HQ Rev.2 shown in Fig. 11. Two cameras are installed at the front of the AUV, while the other two cameras are installed at the bottom.

Fig. 11. IDS UI-3260CP-C-HQ Rev.2

2) DVL (Doppler Velocity Log)

A Teledyne RD Explorer DVL shown in Fig. 12 is used to measure the velocity of the AUV.

Fig. 12. Teledyne DVL.

3) IMU (Inertial Measurement Unit)

The IMU used in Zeabus AUV is a Lord MicroStrain 3DM-GX5-45 shown in Fig. 13, which is mainly used as AHRSs (Altitude Head Reference System).

Fig. 13. Lord MicroStrain 3DM-GX5-45 IMU.

4) Pressure sensor

A pressure sensor used on Zeabus is US331 manufactured by Measurement Specialties shown in Fig. 14. The pressure sensor is used to measure depth of the AUV.

Fig. 14. Pressure sensor.

5) Hydrophone

Four TC 4013 hydrophones made by Teledyne Reson are used to sample an acoustic signal transmitted from a pinger. Four sampled signals will then be processed by a DSP (Digital Signal Processor Board). A TC 4013 hydrophones is shown in Fig. 15.

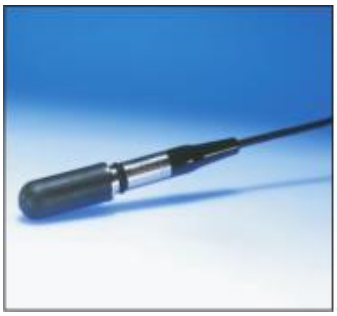

Fig. 15. Teledyne Reson TC 4013 Hydrophone.

6) Imaging sonar

In this year, Teledyne BlueView M900-130 imaging sonar is installed in front of the AUV in order to be used along with cameras for underwater object detection. The imaging sonar is shown in 16.

Fig. 16. Teledyne BlueView M900-130 imaging sonar.

V. Software Design

A. *Software overview*

The Zeabus software system is composed of:

1) Mission planner group module

This part decides a plan, a path, and a direction of the AUV.

2) Control system module

The control system module is used to control thrusters. The main control algorithm used on this module is the PID.

3) Vision system module

The vision system module is used when the AUV has to navigate by using visual data from cameras or imaging sonar.

B. *Mission planner group module*

In mission planner group module shown in Fig. 16, there are several submodules including sensor fusion, mission planner, path planner, and trajectory generator. Sensors, such as IMU, cameras, and hydrophones, send data through communication channels, and then the sensor fusion software module fuses all data together in order to process in the next step. This module also checks the power for operations. The mission planner module uses the fused data to select a strategy to perform tasks based on different criteria. Once the strategy is decided, the path planner module generates the robot path according to the strategy. The trajectory generator then generates actuator trajectories such that the robot will follow the generated path. These trajectories are used as control goals for actuators such as thrusters. Other peripheral devices such as grippers, torpedo launchers, and lamps will be activated based on trajectories generated according to the strategy chosen.

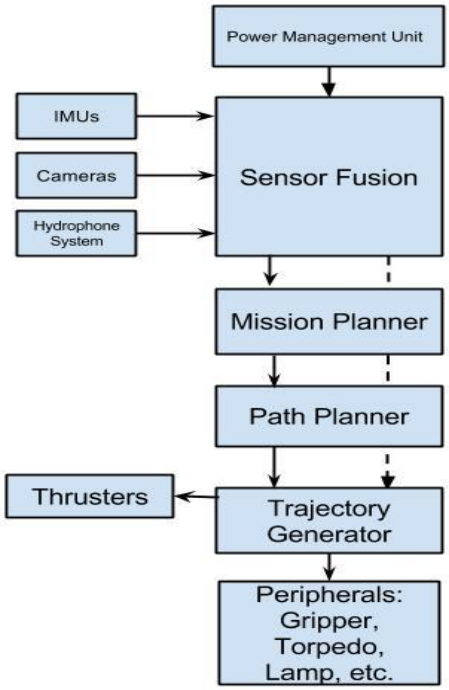

Fig. 16. Mission planner group module.

Our mission planner module is written by Python. Mission planner connects with other systems by ROS (Robot Operating System). When an AUV is performing a task, mission planner acquires and processes data from nodes. After processing, mission planner commands each node to perform the task. This process is repeated until the AUV finishes a task.

C. *Control system module*

A PID control concept [1] shown in Fig. 17 is used to stabilize the depth and heading of our vehicle. The controller receives data from sensor (IMU, DVL, and pressure sensor) and use fusion framework from ROS that estimates position, velocity and attitude of the AUV under the linear system. Here, the location is in Cartesian coordinate whereas the attitude is in the quaternion coordinate. The Unscented Kalman Filter (UKF) [2]. Angle estimates are used to keep track of all AUV positions and attitude. These parameters are used for tuning the PID controls which contains the proportional, integral and derivative terms. Our robot self-stabilizing algorithm uses an estimated angle and the rate of a change in angle. Eight thrusters will be controlled in this process using the pulse width modulation (PWM). Each of the outputs will be carefully calibrated to make the vehicle move in the correct path as much as possible in order to control the robot stability. The control system module also receives command from the PATH controller system where the mission planner module finds the most optimal path for a mission at hand.

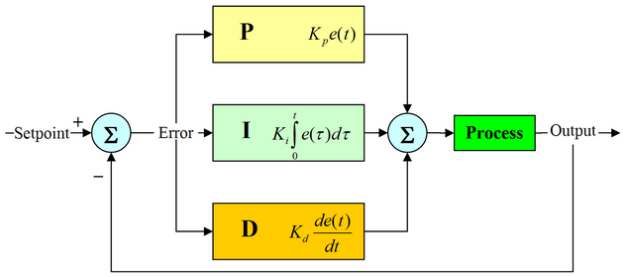

Fig. 17. Block diagram of PID control algorithm

D. *Vision system module*

Our vision system is written by using the OpenCV and the TensorFlow in Python and C++ languages, respectively. The architecture of our vision system module is shown in Fig. 18.

The successful implementation of the proposed system depends on the precise calibration of the cameras to find the suitable exposure. To achieve this goal, we proposed a new idea to merge exposure from two cameras. Fig. 19 displays the flowchart of the exposure merging process. First, the stereo vision is performed on two corresponding images from two cameras with different exposure setting. The same techniques as the high dynamic range (HDR) used in the traditional iPhone cameras is performed. The main reason

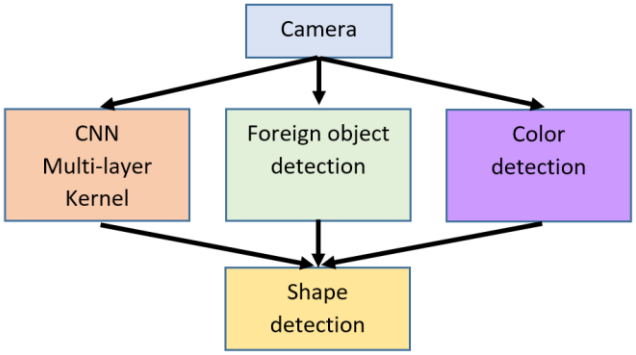

Fig. 18. Vision system architecture.

that we used two cameras instead of one cameras and use it to take images with different exposure is the time delay in exposure setting of the cameras used in our AUV. In Fig. 20, we demonstrated that if the ROS auto exposure is used (upper middle image), the detail of the background cannot be extracted. However, if the images from two different exposure times (upper-left for low exposure and upper-right for high exposure) are combined, we can obtain image with accurate detail (lower-left one) without any saturation.

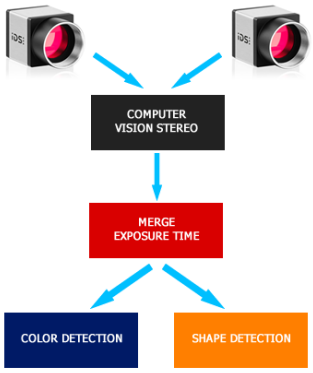

Fig. 19. The flowchart of the exposure merging process.

In the CNN (Convolution Neural Network) [3] module, the image kernel is generated from training data and used to detect and classify which part of the input image from the camera are informative. After that, the image will be segmented for further processing. The segmented images are then passed to Shape detection module to do further processing about the location of that object.

The foreign object detection module will initially detect if there are any objects that should not be in water, on the floor, or in the background. To perform foreign object detection, the captured image is analyzed with the double thresholds [4]. The Average colors of the image are computed so that the color of the "background" can be extracted. This color is then expanded into a range in a color space, which are YUV (or YCbCr) as shown in Fig. 21, in order to decide what is being considered is not an object.

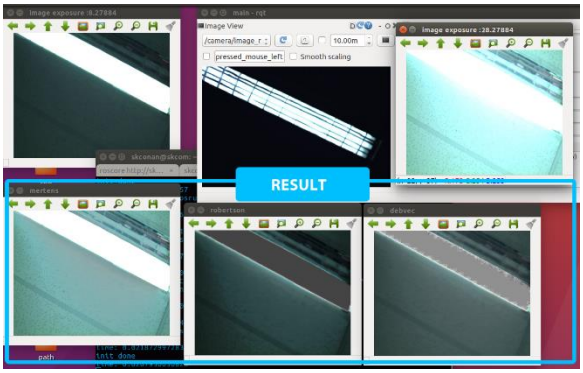

Fig. 20. An example of combining image from two cameras with different exposures.

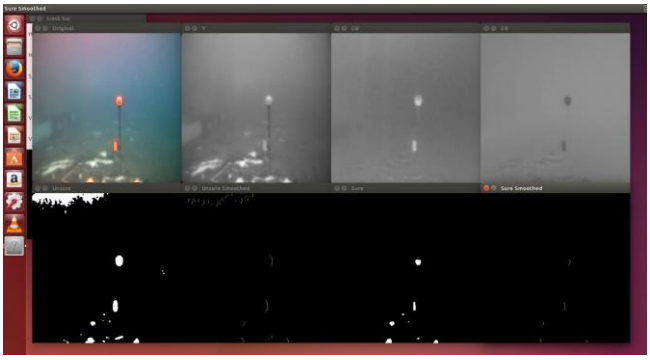

Fig. 21. Buoy in YCbCr color space.

After that, another range is created in order to confirm that the object of interests is an object. By using double thresholds, we can determine an object accurately within a strict range if it is an object of interests or not.

In the top left frame in Fig. 19, the yellow contours drawn over the image mark the part where the algorithm is sure that it is a part of an object. While the red contours mark the actual object that the algorithm recognizes. Since this method is color space independent, it can also be used with the HSV, or even the RGB color space, in case that the YCbCr color space cannot find the defining factor of the object.

The color detection module uses colors that are indexed in the HSV (Hue-Saturation-Value) color space because the HSV allows colors to be represented by only the hue values. After images are acquired from AUV cameras, the imaging data are converted to HSV. The index of colors is obtained by using a user interface shown in Fig. 22 to capture an image and record a range of colors. An example of color detection to detect an underwater gate is shown in Fig. 22. This stage is needed due to a lack of object classification from Foreign object detection.

In the shape detection module, we assumed that a group of pixels has already been detected in an image by extracting desired colors using a color detection algorithm. The

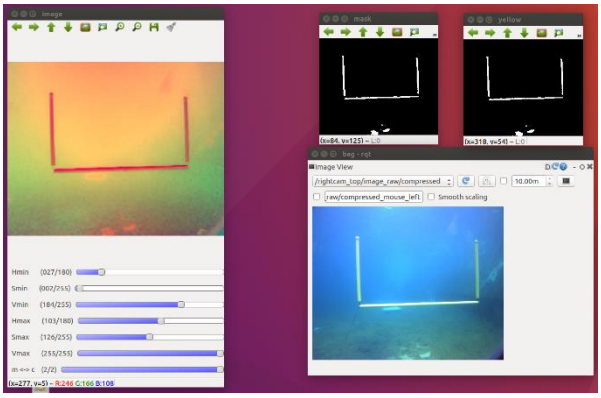

Fig. 22. Vision system interface for gate detection.

detected groups of pixels are called “blob”. Our shape detection algorithm extracts a simple geometric form of an object by using mathematical geometry based on probabilistic and statistical algorithms. An example of shape detection for underwater buoys and path is shown in Fig. 23 and Fig. 24, respectively.

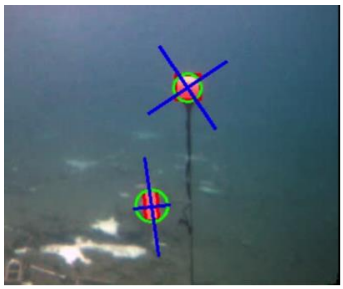

Fig. 23. Shape detection of Buoys

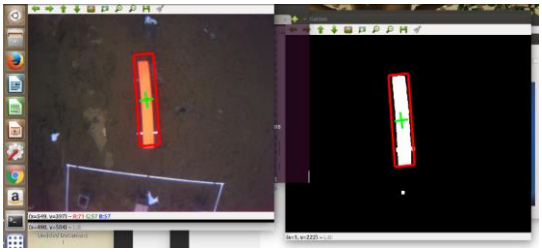

Fig. 24. Shape detection for path determination task.

E. Imaging Sonar

The goal of the imaging sonar is assist the navigation subsystem is finding out the target underwater. The imaging sonar transmits the audio pulses and receives the echo from the surrounding environment. The image is formed from the time-delay, direction of the echo and signal power. The main algorithm to detect and track an object underwater is given in Fig. 25.

In the preprocessing process, the goal is to reduce noise and prepare data for further processing. Here, we only apply the medium filter to reduce the speckle noise. Fig. 26 displays the example of the preprocessing process where the objects are inside the red oval.

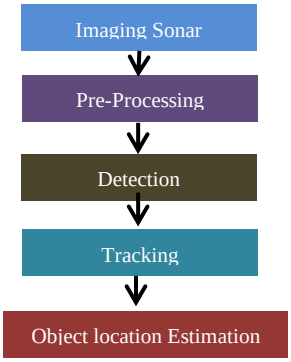

Fig. 25. The block diagram of the imaging sonar module in object tracking

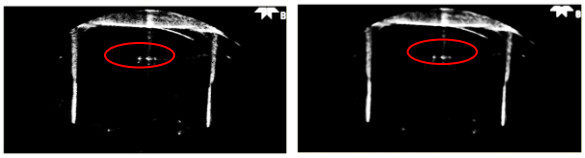

(a) (b)

Fig. 26. Sonar image (a) original image and (b) after medium filter

In the detection step, we apply corner detection to find possible objects in the scene. Fig. 27 displays the corner points of image in Fig. 26 (b). Please note that the corner point detection only performs when the tracking process is enable.

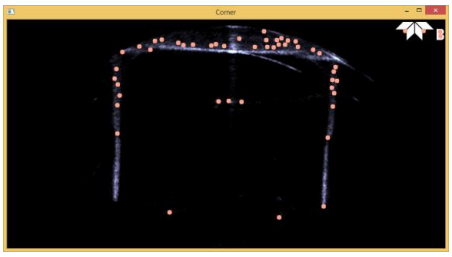

Fig. 27 Detected corner points

For object tracking, we employed the optical flow technique which is based on the work by Lucas and Kanane [7]. Here, they assumed that the similar pixel should move in the similar direction. Hence, they should satisfy the optical flow equations with the same velocities, i.e.,

$$\frac{\partial I}{\partial x}V_x + \frac{\partial I}{\partial y}V_y = -\frac{\partial I}{\partial t} \quad (1)$$

where I is the observed image, and V_x and V_y are local movement of corner points in x- and y-directions. In Fig. 28, the resulting movement of the corner points using the optical flow technique. In the last step, we estimate the object location with respect to the AUV in the polar form.

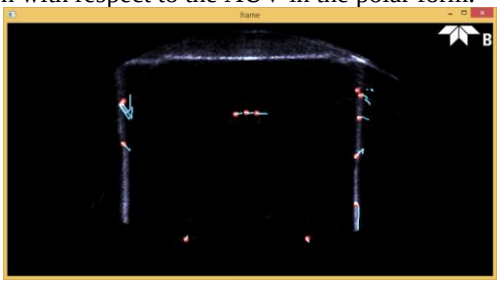

Fig. 28 The movement of direction of the corner points using optical flow technique.

F. Hydrophone processing module

Our hydrophone processing module is designed for searching an acoustic signal from the pinger. The detector is mounted under the AUV platform to measure wave heights and periods from four hydrophones as input signals. The signals are amplified before being analyzed. Location output data are then provided. The localization configuration is shown in Fig. 29.

The software methodology for hydrophones carries out six steps:

1) Sampling

This step is the beginning of the processing where the analog signal is converted to a digital signal.

2) Bandpass filtering

Since the pinger signals is a monotonic with frequencies ranging from 25 to 40 kHz. We decided to perform a digital bandpass filter. Here, the infinite impulse response (IIR) filter is employed due to its simplicity and speedy computation.

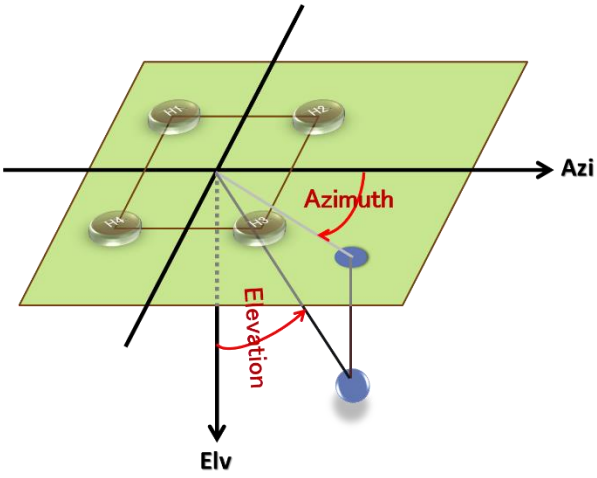

Fig. 29. Localization scenario with 4 hydrophones

3) Pulse detection and demodulation

This step is used to detect the pinger pulses where they will be demodulated to a baseband signal. There are two thresholds used in the process, front and power thresholds.

- The front threshold is a fixed value to be set at the larger values than the background noise. We have the front threshold to reduce unnecessary load in the system. In Fig. 30, the example of the pinger signal under the presence of noise is demonstrated. Here, the signal pulse is detected at the 251-st sample.
- The power threshold is designed to make sure that the detected pulse is a real signal. Here, we the moving average on all hydrophone channels to estimate noise power if, in all channels, there is significant increase of the received signal, the power threshold will say a pulse is detected and the pinger bearing estimation process is called.

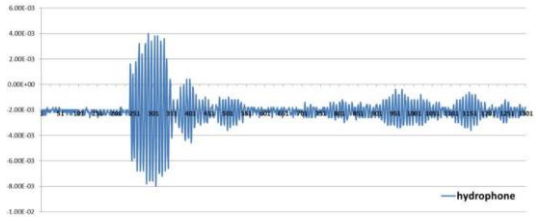

Fig. 30. The pinger signal with noise background

4) Pinger pulse frequency estimation

In the stage, our goal is to estimate the frequency of the transmitted pinger pulse. The fast Fourier transform (FFT) is applied to the detected pulses where the pinger frequency is associated with the frequency with the largest magnitude.

5) Delay time estimation.

Since the pulse detection algorithm may not be perfect, and the pinger signal may arrive at hydrophone from different directions and time delays due to multipath nature of underwater sound propagation, the delay-time estimation is used to accurately extract the first arrival pulse of the pinger signal from all four hydrophones for further processing. Here, we assume that the line-of-sight is the shortest path between pinger and hydrophones.

6) Bearing estimation

The azimuth angle and the elevation angle are computed in this step as the output of the system. Here, we measure the phase differences of the arrival signals at all hydrophones. If a pinger is on the right, the phase of the received signals of the right hydrophone should lead the hydrophone on the left. In fact, we have

$$\psi_i = \frac{2\pi}{\lambda} f_i(\phi, \theta) \qquad (2)$$

where ψ_i is the phase delay at the i-th hydrophone, λ is the wavelength of the pinger pulse, ϕ is the azimuth angle, θ is the elevation angle, and $f_i(.,.)$ is a function that depends on the geometry of hydrophones with respect to the AUV axes. Table I demonstrate the accuracy of our system for different bearing angles. We found that our technique can estimate bearing of the hydrophone quite accurately.

Table I: Experimental results of Pinger bearing estimation

	Case 1		Case 2		Case 3	
	ϕ	θ	ϕ	θ	ϕ	θ
Actual	30	26	75	38	70	38
Estimated	31.8	22.7	65.8	34.0	65.2	68.1

VI. Conclusion

In this team description paper, a design of Zeabus AUV was described. Technical details of designs on mechanical, electrical, and software parts were covered. Unfortunately, we could not finish our vision system yet so only hydrophone system results can imply the capability of our system. Our AUV is being improved much compared to the last year. This is a good opportunity for students in the team to learn several advance algorithms and implementation with respect to their

education levels. However, there are still many details that we still want to improve for better performance. We plan to implement that in Robosub 2017 too.

ACKNOWLEDGEMENT

Zeabus AUV team has to thank many sponsors. Our highly respected main sponsors are Faculty of Engineering, Kasetsart University and PTTEP, which provides us financial supports. We appreciate staffs from Hiveground, Co. Ltd., and EmOne, Co. Ltd., for their advices to our students. Finally, we thank Kasetsart University for providing us time and space to use a university diving pool.

REFERENCES

[1] T. I. Fossen, "Motion control system," in *Handbook of Marine Craft Hydrodynamics and Motion Control*, 1th ed. West Sussex, UK: Wiley, 2011, ch. 12, sec. 2, pp. 365-398.

[2] E. A. Wan and R. Van Der Merwe, "The unscented Kalman filter for nonlinear estimation," *IEEE AS-SPCC*, Lake Louise, AB, Canada, 2000, pp. 153-158.

[3] A. Krizhevsky, I. Sutskever, and G. E. Hinton, "Imagenet classification with deep convolutional neural networks," *Advances in neural information processing systems*. 2012, pp. 1097-1105.

[4] J. Canny. "A computational approach to edge detection" *IEEE Trans. PAMI*, vol. 8, no. 6, pp. 679–698, Nov. 1986.

[5] P. Panagiotou, A. Polydoros, and P. Thiennviboon, "Multiple-Path Direction-of-Arrival Estimation for Cognitive Radio Sensing," *The 21st Annual IEEE International Symposium on Personal, Indoor, and Mobile Radio Communication*, Istanbul, 2010, pp. 791-796.

[6] M. S. Arulampalam, S. Maskell, N. Gordon, and T. Clapp, "A tutorial on particle filters for online nonlinear/non-Gaussian Bayesian tracking," *IEEE Trans. Signal Processing*, vol. 50, no. 2, pp. 174-188, Feb. 2002.

[7] B. D. Lucas and T. Kanade (1981), "An iterative image registration technique with an application to stereo vision," *Proceedings of Imaging Understanding Workshop*, pages 121-130, 1981

.